Determination of α_S from azimuthal correlations among jets

Paris Gianneios

on behalf of the CMS Collaboration

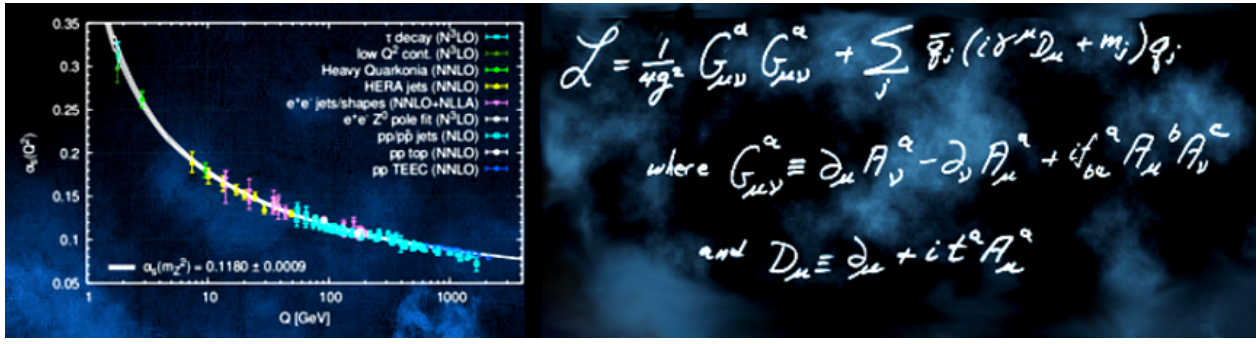

alphas-2024: Workshop on precision measurements of the QCD coupling constant, ECT*, Trento

iihe BRUXELLES BRUSSEL

ULB UNIVERSITÉ LIBRE DE BRUXELLES

CMS

Outline

1. Motivation: α_S from angular/azimuthal correlations among jets
   - D0 $\rightarrow R_{\Delta R}$ observable, (2012) $\sqrt{s} = 1.96$ TeV (10.1016/j.physletb.2012.10.003)
   - ATLAS $\rightarrow R_{\Delta\phi}$ observable, (2018) $\sqrt{s} = 8$ TeV (10.1103/PhysRevD.98.092004)
   - CMS $\rightarrow R_{\Delta\phi}$ observable, (2024) $\sqrt{s} = 13$ TeV (CMS-PAS-SMP-22-005)

2. CMS results: determination of α_S using $R_{\Delta\phi}$ observable
   - Measurement
   - Theoretical predictions
   - Determination of $\alpha_S(M_Z)$
   - Investigation of $\alpha_S(Q)$ evolution

Motivation

Multijet cross section ratios

Goals

1. Determination of $\alpha_S(M_Z)$.
2. Investigation of $\alpha_S(Q)$ running.

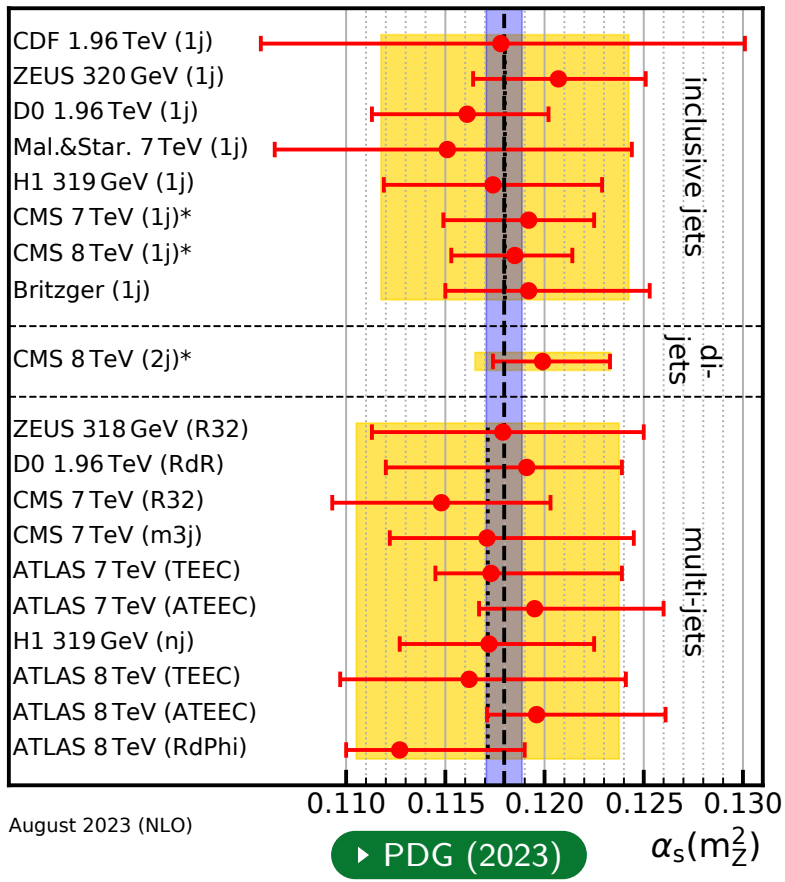

Motivation

Multijet cross section ratios

Goals

1. Determination of $\alpha_S(M_Z)$.
2. Investigation of $\alpha_S(Q)$ running.

Observables: Ratios (R) with

- **Denominator: topologies with at least 2-jets.**

$R =$ 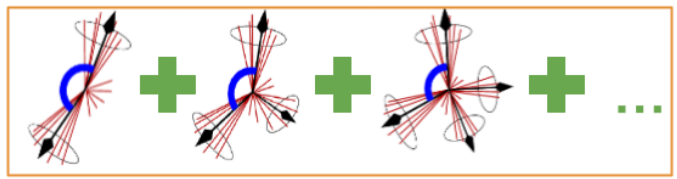

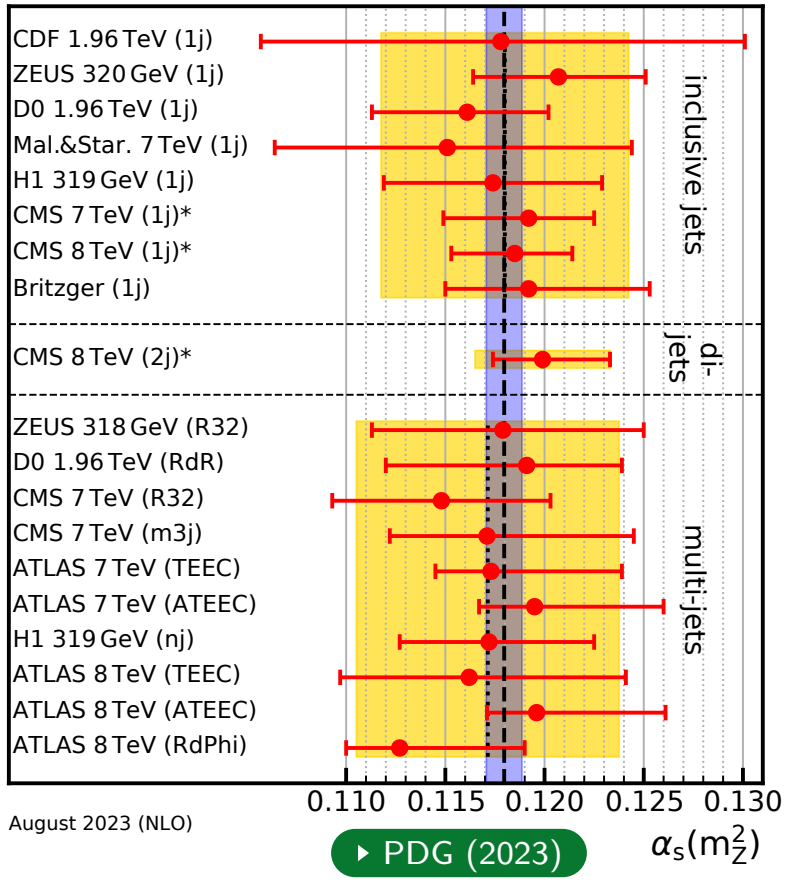

Motivation

Multijet cross section ratios

Goals

1. Determination of $\alpha_S(M_Z)$.
2. Investigation of $\alpha_S(Q)$ running.

Observables: Ratios (R) with

- **Denominator: topologies with at least 2-jets.**
- **Numerator: topologies with at least 3-jets enforced using angular/azimuthal criteria.**

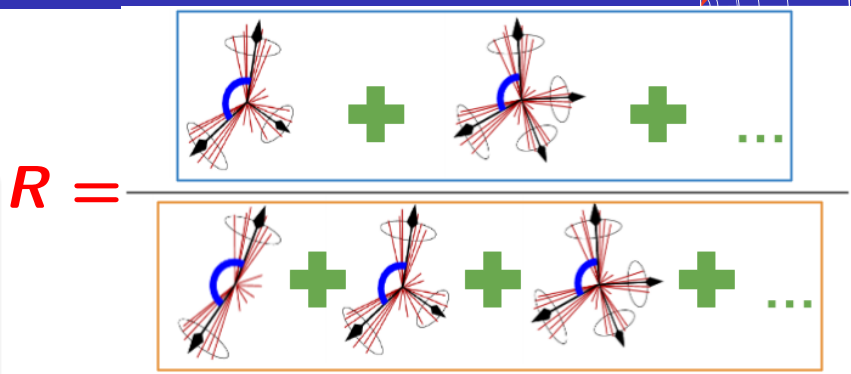

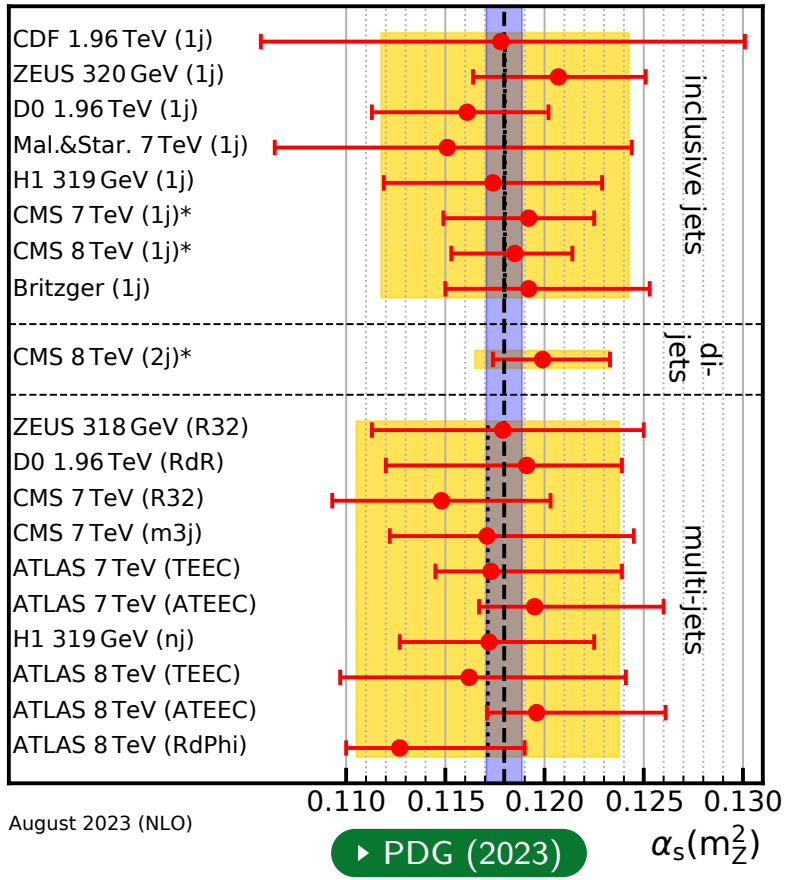

Motivation

Multijet cross section ratios

Goals

1. Determination of $\alpha_S(M_Z)$.
2. Investigation of $\alpha_S(Q)$ running.

Observables: Ratios (R) with

- **Denominator: topologies with at least 2-jets.**
- **Numerator: topologies with at least 3-jets enforced using angular/azimuthal criteria.**

Benefits

✔ Reduction/cancellation of experimental uncertainties e.g. luminosity.

✔ Reduction of theoretical uncertainties e.g. PDF.

$R =$ 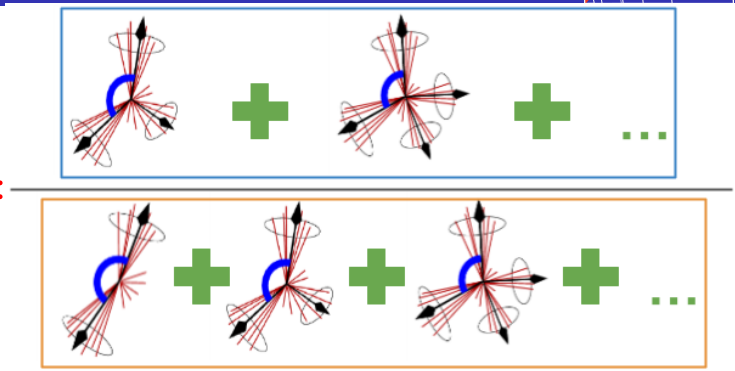

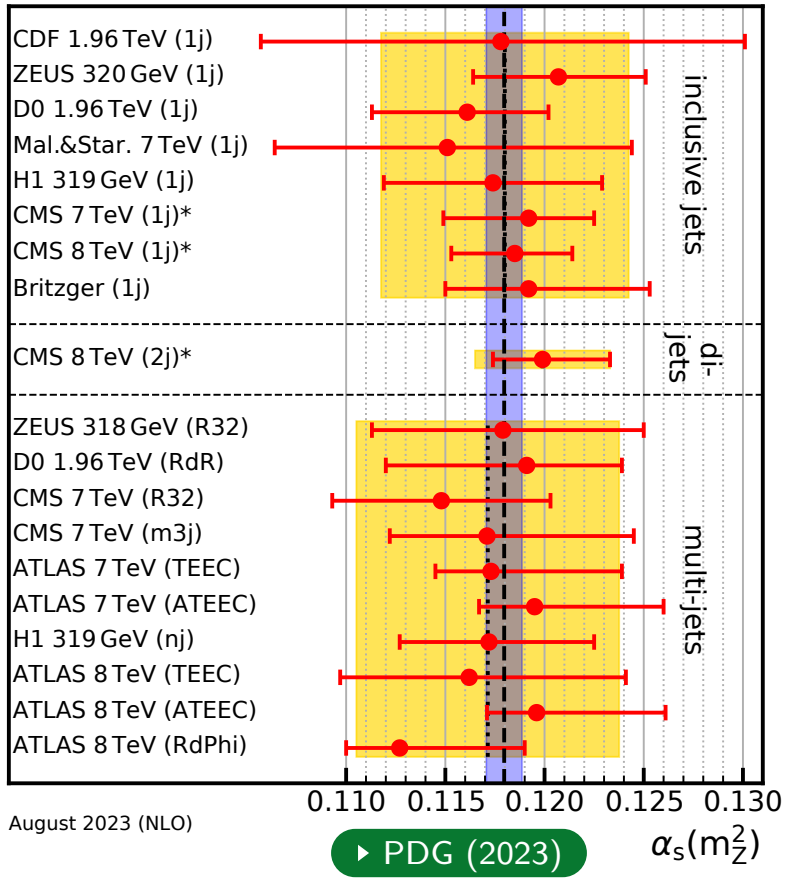

Motivation

Multijet cross section ratios

Goals

1. Determination of $\alpha_S(M_Z)$.
2. Investigation of $\alpha_S(Q)$ running.

Observables: Ratios (R) with

- **Denominator: topologies with at least 2-jets.**
- **Numerator: topologies with at least 3-jets enforced using angular/azimuthal criteria.**

Benefits

✔ Reduction/cancellation of experimental uncertainties e.g. luminosity.

✔ Reduction of theoretical uncertainties e.g. PDF.

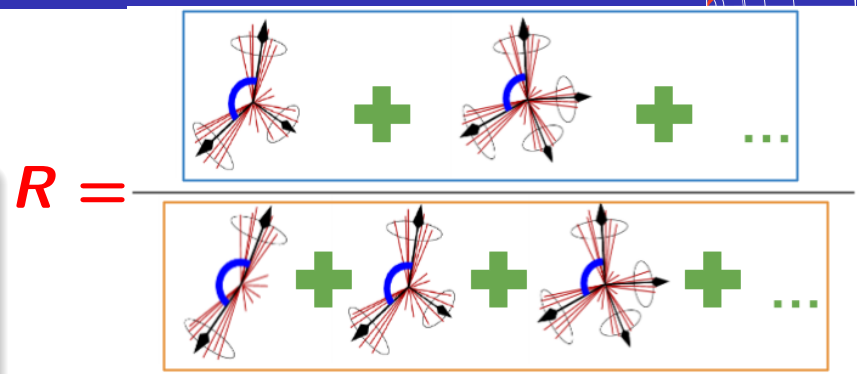

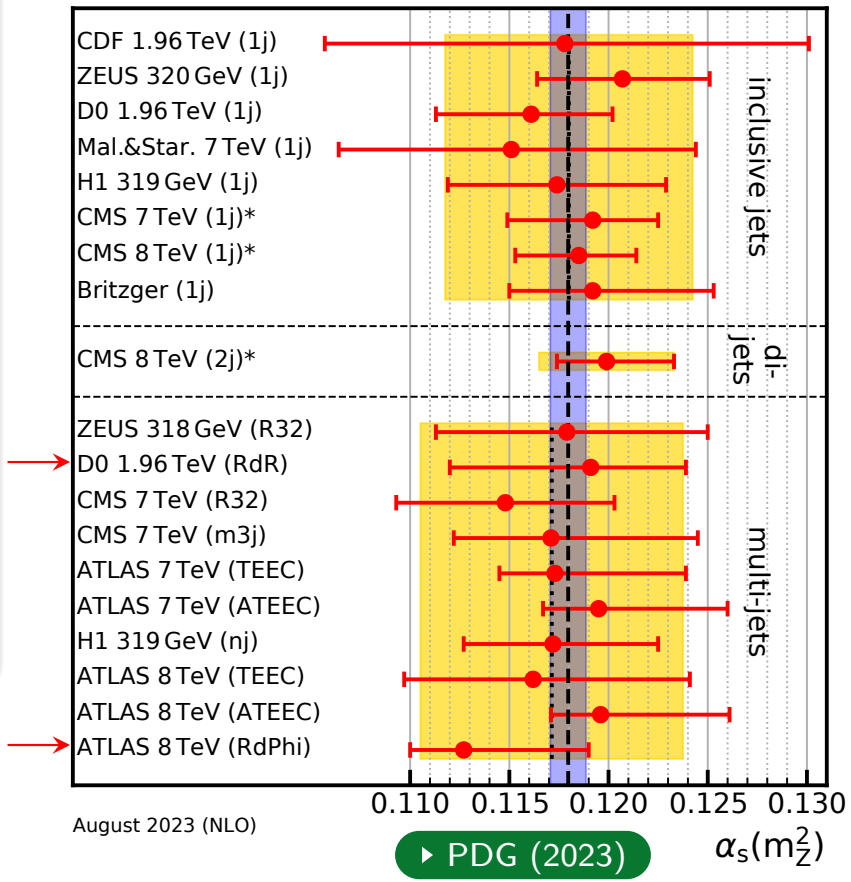

(D0) $R_{\Delta R}$ definition

$$R_{\Delta R} = \frac{\sum_{i=1}^{N_{jet}(p_T)} N_{nbr}^{(i)}(\Delta R, p_{Tmin}^{nbr})}{N_{jet}(p_T)}$$

- N_{jet}: inclusive number of jets.
- N_{nbr}: jets with neighbours within angular separation interval ΔR and $p_T > p_{Tmin}^{nbr}$.

▸ 10.1016/j.physletb.2012.10.003, $(p\bar{p})$ $\sqrt{s} = 1.96$ TeV

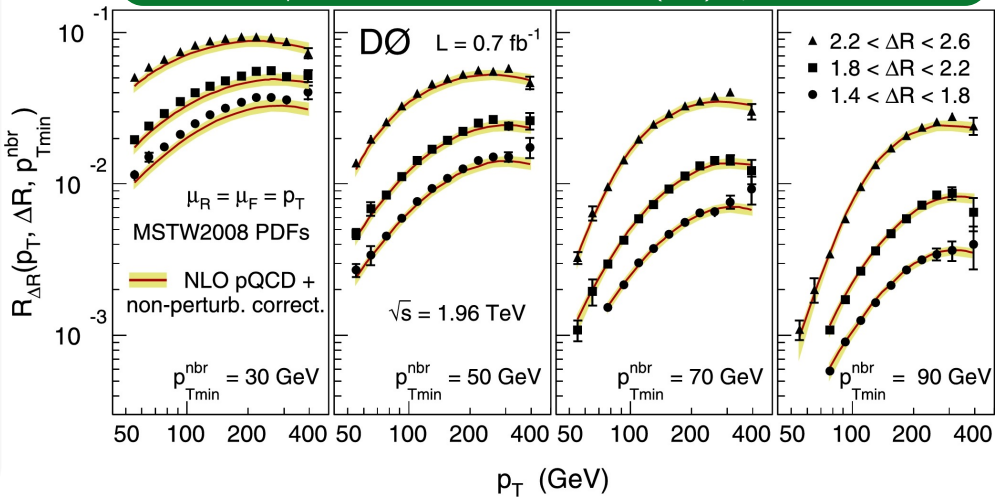

$R_{\Delta R}$ and $R_{\Delta\phi}$ observables

(D0) $R_{\Delta R}$ definition

$$R_{\Delta R} = \frac{\sum_{i=1}^{N_{jet}(p_T)} N_{nbr}^{(i)}(\Delta R, p_{Tmin}^{nbr})}{N_{jet}(p_T)}$$

- N_{jet}: inclusive number of jets.
- N_{nbr}: jets with neighbours within angular separation interval ΔR and $p_T > p_{Tmin}^{nbr}$.

▸ 10.1016/j.physletb.2012.10.003, $(p\bar{p})$ $\sqrt{s} = 1.96$ TeV

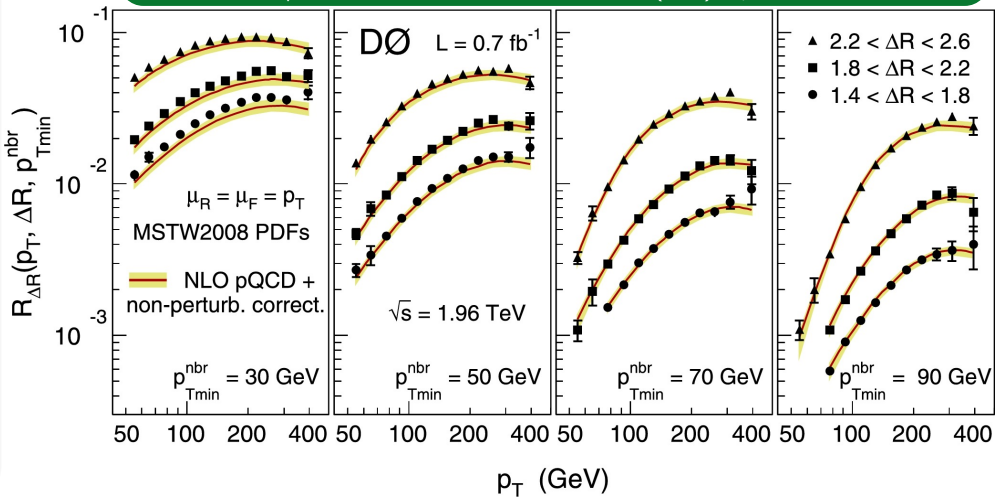

(ATLAS) $R_{\Delta\phi}$ definition

$$R_{\Delta\phi} = \frac{\frac{d^2\sigma_{dijet}(\Delta\phi_{dijet} < \Delta\phi_{max})}{dH_T\, dy^*}}{\frac{d^2\sigma_{dijet}(inclusive)}{dH_T\, dy^*}}$$

- σ_{dijet}: inclusive dijet sample.
- H_T: $\sum_{i\in\text{jets}} p_{T,i}$, y^*: $|y_1 - y_2|/2$.

▸ 10.1103/PhysRevD.98.092004, (pp) $\sqrt{s} = 8$ TeV

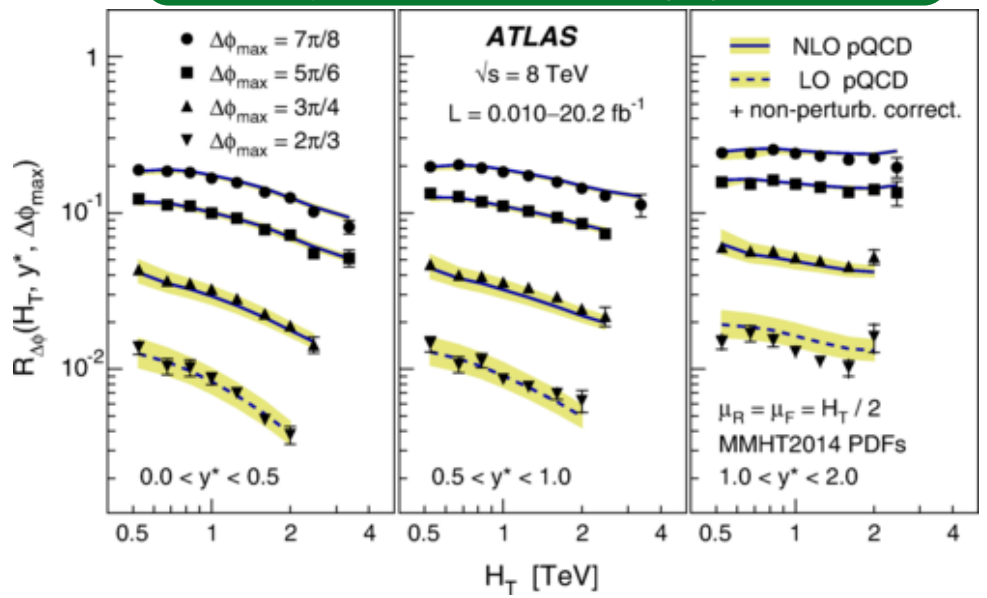

CMS: $R_{\Delta\phi}$ observable

$$R_{\Delta\phi} = \frac{}{N_{jet}(p_T)}$$

Number of jets in a jet p_T bin ($\sim \alpha_s^2$ @LO)

2-jet topology

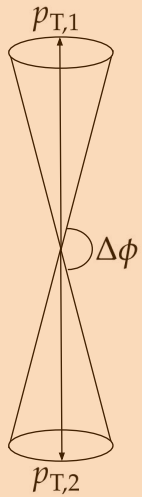

$R_{\Delta\phi}(p_T)$ **entries**

$\Delta\phi \approx \pi$

Numerator: 0

Denominator: 2

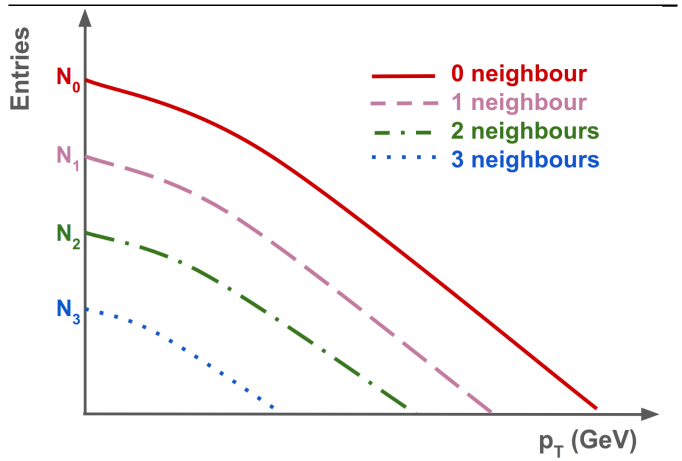

CMS: $R_{\Delta\phi}$ observable

Jets with neighbours within azimuthal separation:
$2\pi/3 < \Delta\phi < 7\pi/8$ and $p_T > 100$ GeV ($\sim \alpha_s^3$ @LO)

$$R_{\Delta\phi} = \frac{\sum_{i=1}^{N_{jet}(p_T)} N_{nbr}^{(i)}(\Delta\phi, p_{Tmin}^{nbr})}{N_{jet}(p_T)}$$

Number of jets in a jet p_T bin ($\sim \alpha_s^2$ @LO)

2-jet topology	3-jet topology (all jets with $p_T > 100$ GeV)
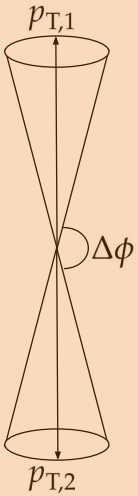	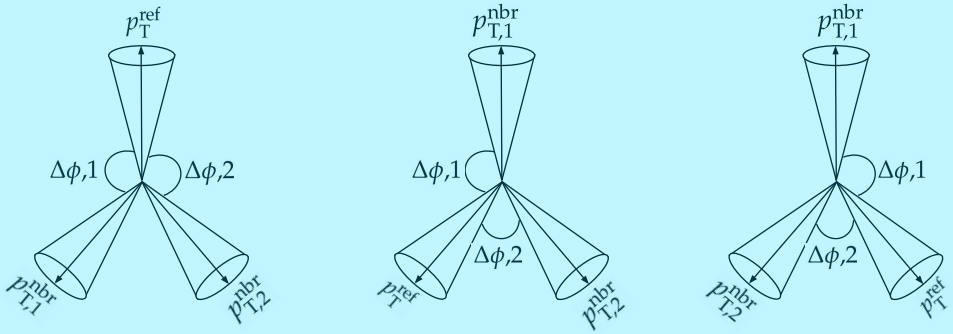
$R_{\Delta\phi}(p_T)$ entries $\Delta\phi \approx \pi$ Numerator: 0 Denominator: 2	$R_{\Delta\phi}(p_T)$ entries Numerator: 2 $2\pi/3 < \Delta\phi,1 < 7\pi/8$ $2\pi/3 < \Delta\phi,2 < 7\pi/8$ + Numerator: 1 $2\pi/3 < \Delta\phi,1 < 7\pi/8$ $\Delta\phi,2 < 2\pi/3$ + Numerator: 1 $2\pi/3 < \Delta\phi,1 < 7\pi/8$ $\Delta\phi,2 < 2\pi/3$ Denominator: 3

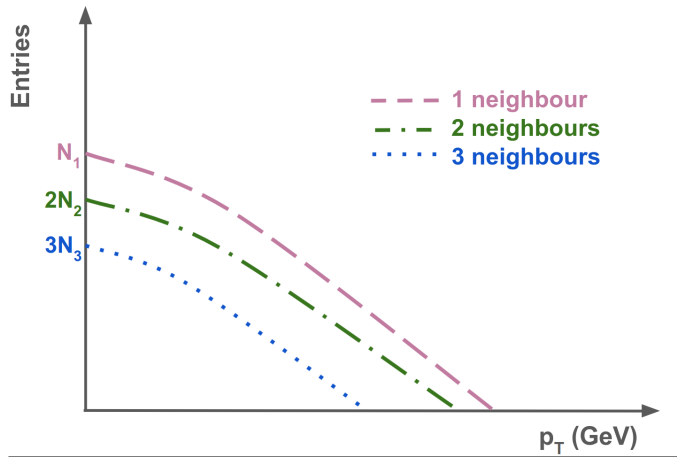

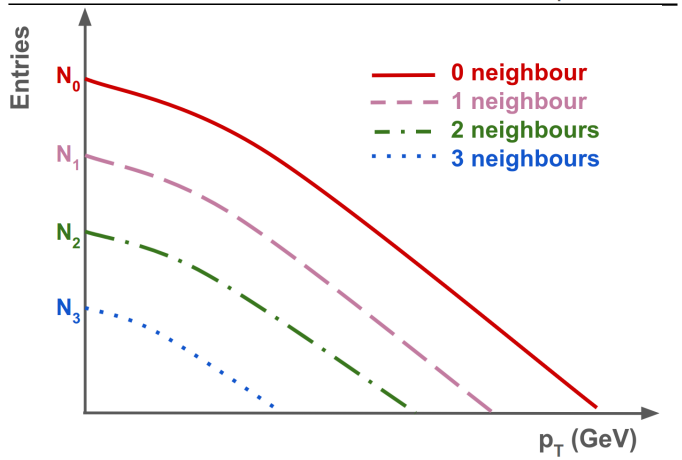

CMS: $R_{\Delta\phi}$ observable

Experimental data

- Full Run 2: $\mathcal{L}_{int} = 134\ fb^{-1}$
- Event sample with jets:
  - **anti-k_T** with $R = 0.7$
  - $p_T > 50\ GeV$, $|y| < 2.5$
- Numerator selection criteria:
  - $(\Delta\phi_{min}, \Delta\phi_{max}) = (2\pi/3, 7\pi/8)$
  - $p_{Tmin}^{nbr} = 100\ GeV$

Results from: ▸ CMS-PAS-SMP-22-005

CMS: $R_{\Delta\phi}$ observable

Experimental data

- Full Run 2: $\mathcal{L}_{int} = 134\ fb^{-1}$
- Event sample with jets:
  - **anti-k_T** with $R = 0.7$
  - $p_T > 50\ GeV$, $|y| < 2.5$
- Numerator selection criteria:
  - $(\Delta\phi_{min}, \Delta\phi_{max}) = (2\pi/3, 7\pi/8)$
  - $p_{Tmin}^{nbr} = 100\ GeV$

Theoretical predictions

- Fixed-order predictions pQCD @NLO.
- **NLOJet++** (up to 3 jets @NLO)
- Using the fastNLO framework.
- $\mu_R = \mu_F = \hat{H}_T/2$,
  with $\hat{H}_T = \sum_{i \in \text{partons}} p_{T,i}$

Results from: CMS-PAS-SMP-22-005

CMS: $R_{\Delta\phi}$ observable

Experimental data

- Full Run 2: $\mathcal{L}_{int} = 134\ fb^{-1}$
- Event sample with jets:
  - **anti-k_T** with $R = 0.7$
  - $p_T > 50\ GeV$, $|y| < 2.5$
- Numerator selection criteria:
  - $(\Delta\phi_{min}, \Delta\phi_{max}) = (2\pi/3, 7\pi/8)$
  - $p_{Tmin}^{nbr} = 100\ GeV$

Theoretical predictions

- Fixed-order predictions pQCD @NLO.
- **NLOJet++** (up to 3 jets @NLO)
- Using the fastNLO framework.
- $\mu_R = \mu_F = \hat{H}_T/2$, with $\hat{H}_T = \sum_{i \in \text{partons}} p_{T,i}$

Results from: CMS-PAS-SMP-22-005

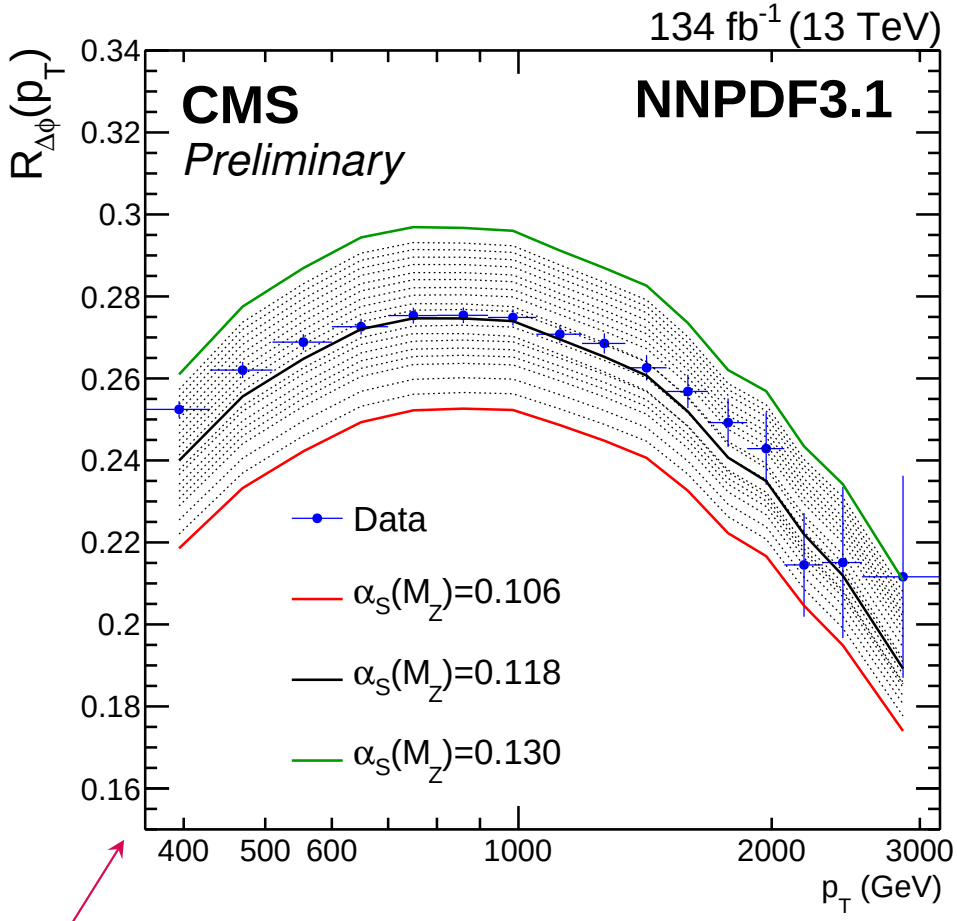

$R_{\Delta\phi}$ observable has large sensitivity to α_S.

Measurement: Unfolding

- **Data Unfolding:** correct the measurement for the detector smearing effects.
- **TUnfold package:** least square minimisation without Tikhonov regularisation:

$$\chi^2 = (Ax + b - y)^T V^{-1} (Ax + b - y)$$

Measurement: Unfolding

- **Data Unfolding:** correct the measurement for the detector smearing effects.
- **TUnfold package:** least square minimisation without Tikhonov regularisation:

$$\chi^2 = (Ax + b - y)^T V^{-1} (Ax + b - y)$$

- Equivalent observable definition using 2D $N(p_T, n)$ distribution:

$$\boldsymbol{R_{\Delta\phi} = \frac{\sum_{i=1}^{N_{jet}(p_T)} N_{nbr}^{(i)}(\Delta\phi, p_{Tmin}^{nbr})}{N_{jet}(p_T)} = \frac{\sum_{n=0}^{\infty} nN(p_T, n)}{\sum_{n=0}^{\infty} N(p_T, n)}}$$

where $\boldsymbol{n}$ is the number of neighbours and $\boldsymbol{p_T}$ is jet's transverse momentum.

Measurement: Unfolding

- **Data Unfolding:** correct the measurement for the detector smearing effects.
- **TUnfold package:** least square minimisation without Tikhonov regularisation:

$$\chi^2 = (Ax + b - y)^T V^{-1} (Ax + b - y)$$

- Equivalent observable definition using 2D $N(p_T, n)$ distribution:

$$\boldsymbol{R_{\Delta\phi} = \frac{\sum_{i=1}^{N_{jet}(p_T)} N_{nbr}^{(i)}(\Delta\phi, p_{Tmin}^{nbr})}{N_{jet}(p_T)} = \frac{\sum_{n=0}^{\infty} nN(p_T, n)}{\sum_{n=0}^{\infty} N(p_T, n)}}$$

where $\boldsymbol{n}$ is the number of neighbours and $\boldsymbol{p_T}$ is jet's transverse momentum.

Motivation

👉 Multidimensional unfolding of the $N(p_T, n)$ distribution.

✔ Account for migrations among p_T bins **and** among n bins.

✔ Account for non-trivial correlations between the numerator and denominator.

Measurement: Unfolding

Probability matrix for the 2D $N(p_T, n)$

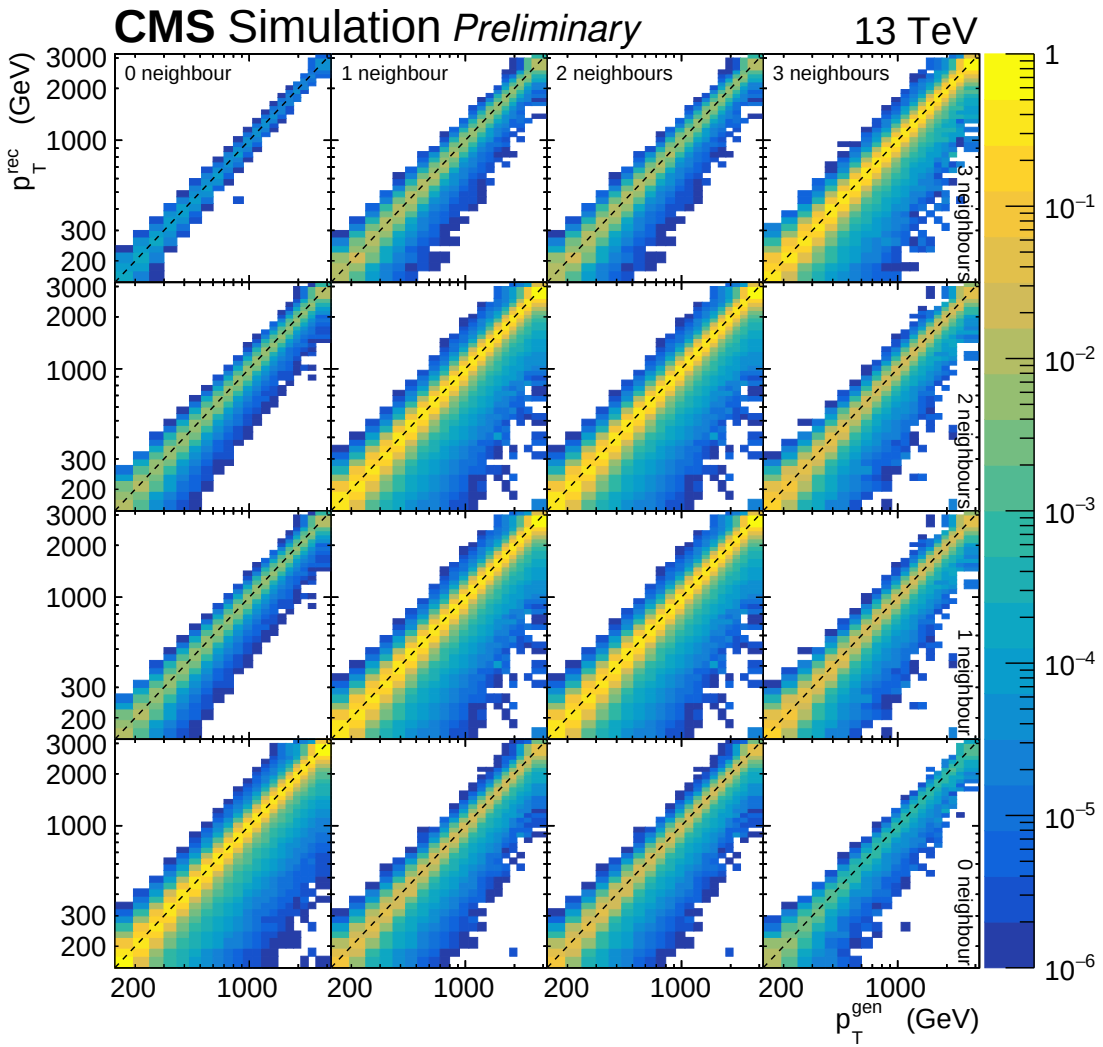

- Probability matrix built using Pythia8.
  - x axis: generator-level p_T.
  - y axis: reconstructed-level p_T.
  - inner cells: neighbouring jet bins.
- Model uncertainties ($< 0.01\%$) investigated using alternative MC models (Madgraph).

Measurement: Uncertainties

Statistical correlation matrix for $R_{\Delta\phi}$ *after* unfolding

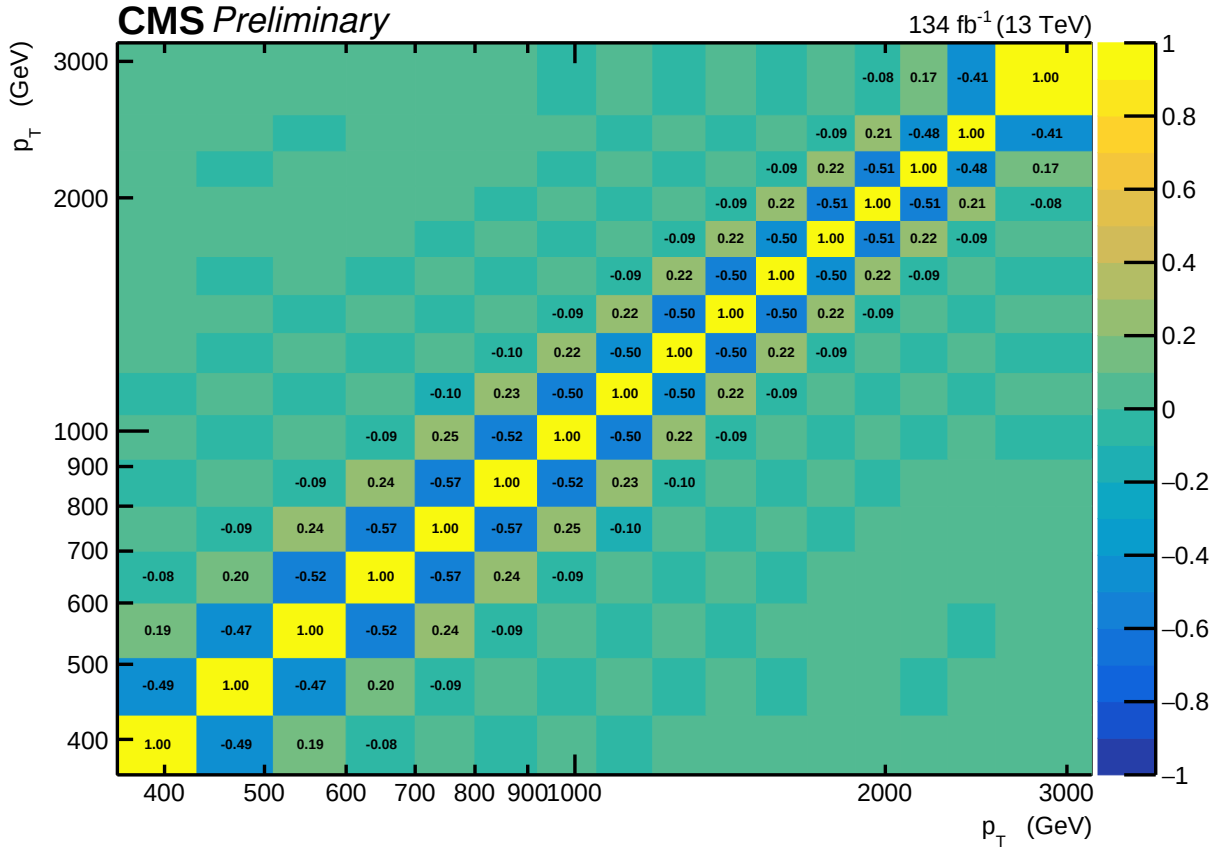

- **Statistical** ($< 11\%$): from the covariance matrix *after* unfolding.
- **JES** ($< 5\%$): **J**et **E**nergy **S**cale uncertainty sources $\rightarrow p_T = p_T(1 \pm \text{unc. source})$.
- **JER** ($< 0.8\%$): **J**et **E**nergy **R**esolution smearing process applied to MC samples.
- **Other** ($< 1\%$): Prefiring corrections, PU profile reweighting, MC modeling.

Monte Carlo predictions

- Predictions from MC event generators at particle level using RIVET toolkit.
  - For the comparison with experimental data.
  - For the evaluation of non-perturbative (NP) effects.

Monte Carlo predictions

- Predictions from MC event generators at particle level using RIVET toolkit.
  - For the comparison with experimental data.
  - For the evaluation of non-perturbative (NP) effects.

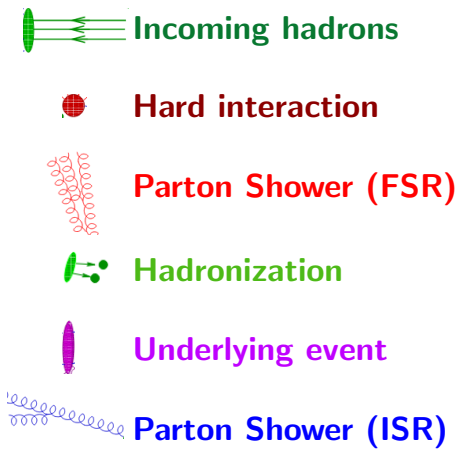

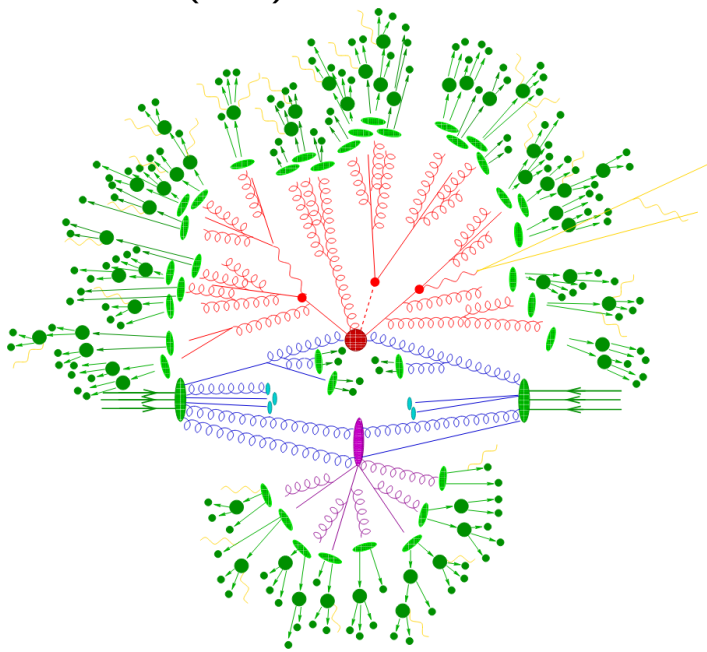

MC	Matrix Element	Parton Shower	Hadronization	Tune	PDF set
PYTHIA8	$2 \to 2$ (LO)	p_T ordered	Lund string	CUETP8M1	NNPDF2.3
				CUETP8M2	NNPDF3.0
HERWIG++	$2 \to 2$ (LO)	Angular ordered	Cluster model	EE5C	CTEQ6.1M
POWHEG	$2 \to 2$ (NLO), $2 \to 3$ (LO)	PYTHIA8	PYTHIA8	CUETP8M1	NNPDF3.0
		PYTHIA8	PYTHIA8	CUETP8M2	NNPDF3.0
		HERWIG++	HERWIG++	EE5C	NNPDF3.0

Monte Carlo predictions

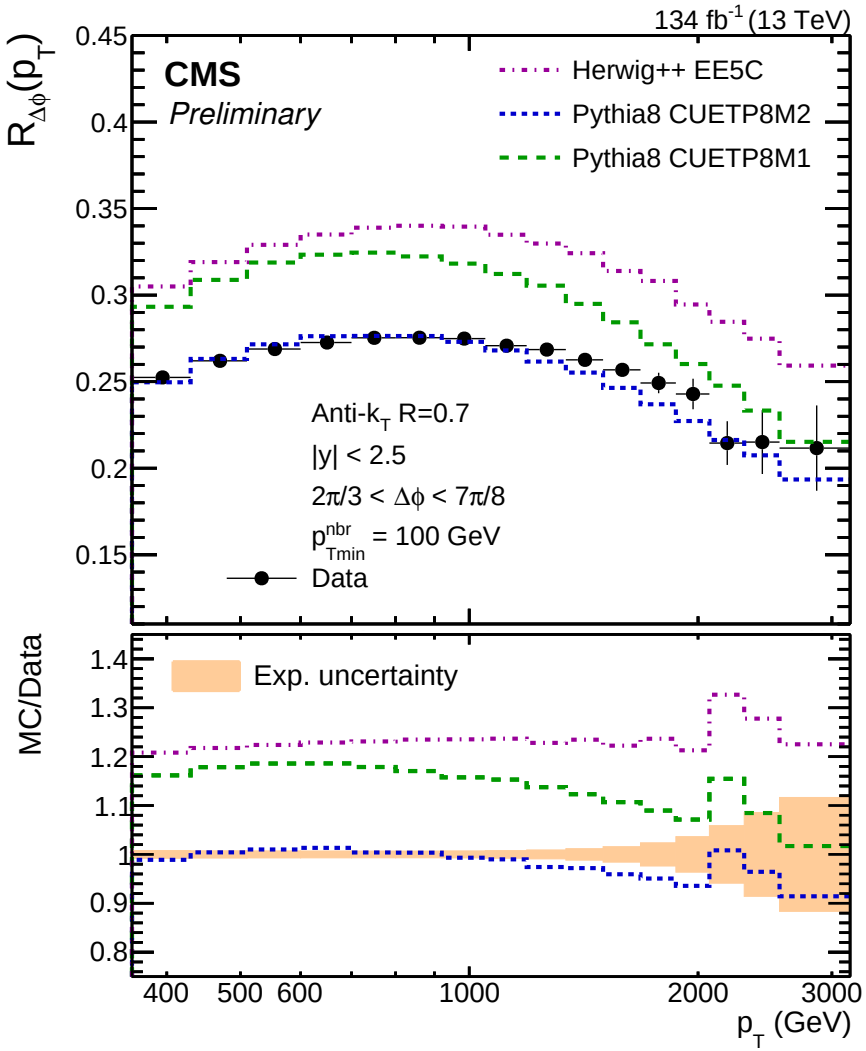

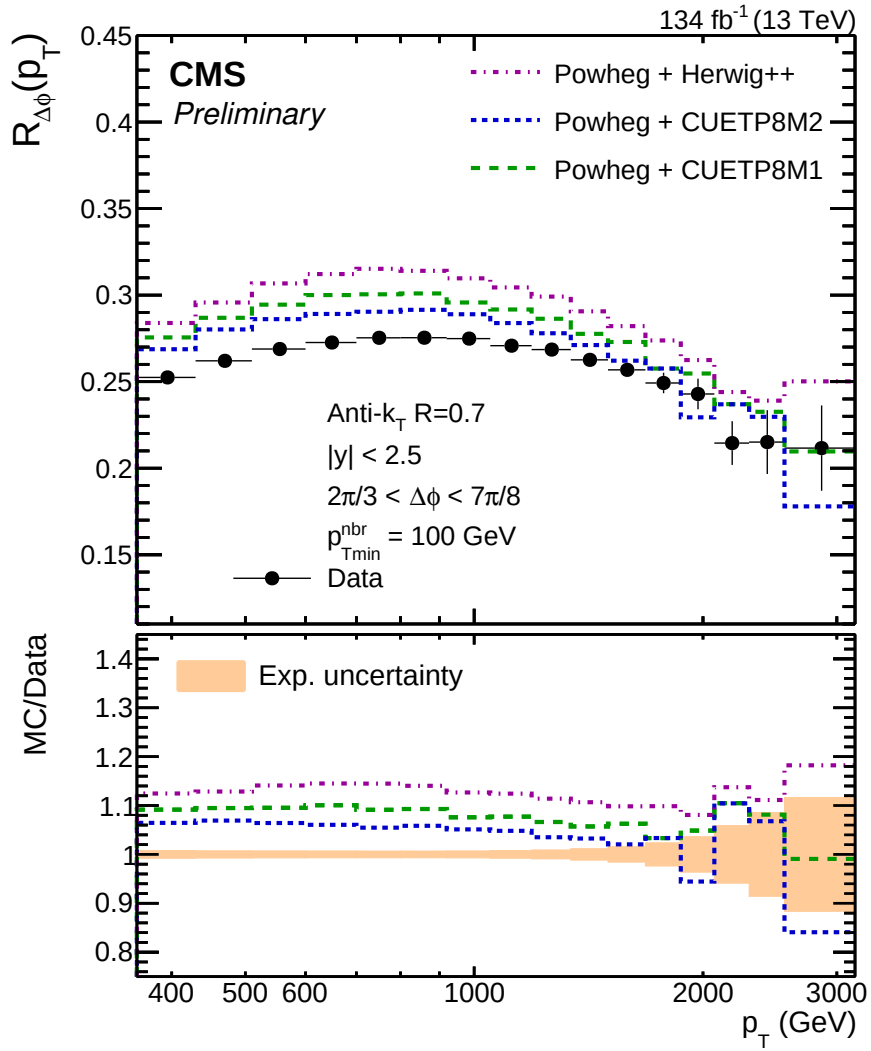

- Predictions from Powheg overestimate the measurement by ∼5-12%.
- Herwig++ EE5C (Pythia8 CUETP8M1) overestimate $R_{\Delta\phi}$ by ∼ 20% (∼12-18%).
- Nice description from (LO) Pythia8 tune CUETP8M2T4.

Fixed Order pQCD

- **Fixed-order pQCD predictions @NLO**
  - 4 different PDF sets.
- **PDF uncertainties**
  - 68% CL Hessian/MC methods.
- **Scale uncertainties**
  - $\frac{1}{2} \leq \mu_R/\mu_F \leq 2$

PDFs available via LHAPDF

PDF set	Default $\alpha_s(M_Z)$	Alternative $\alpha_s(M_Z)$
ABMP16	0.1191	0.114 - 0.123
CT18	0.1180	0.110 - 0.124
MSHT20	0.1200	0.108 - 0.130
NNPDF3.1	0.1180	0.106 - 0.130

Fixed Order pQCD

- **Fixed-order pQCD predictions @NLO**
  - 4 different PDF sets.
- **PDF uncertainties**
  - 68% CL Hessian/MC methods.
- **Scale uncertainties**
  - $\frac{1}{2} \leq \mu_R/\mu_F \leq 2$

PDFs available via LHAPDF

PDF set	Default $\alpha_s(M_Z)$	Alternative $\alpha_s(M_Z)$
ABMP16	0.1191	0.114 - 0.123
CT18	0.1180	0.110 - 0.124
MSHT20	0.1200	0.108 - 0.130
NNPDF3.1	0.1180	0.106 - 0.130

NLO scale uncertainties

Numerator: 9-17%
Denominator: 5-10%

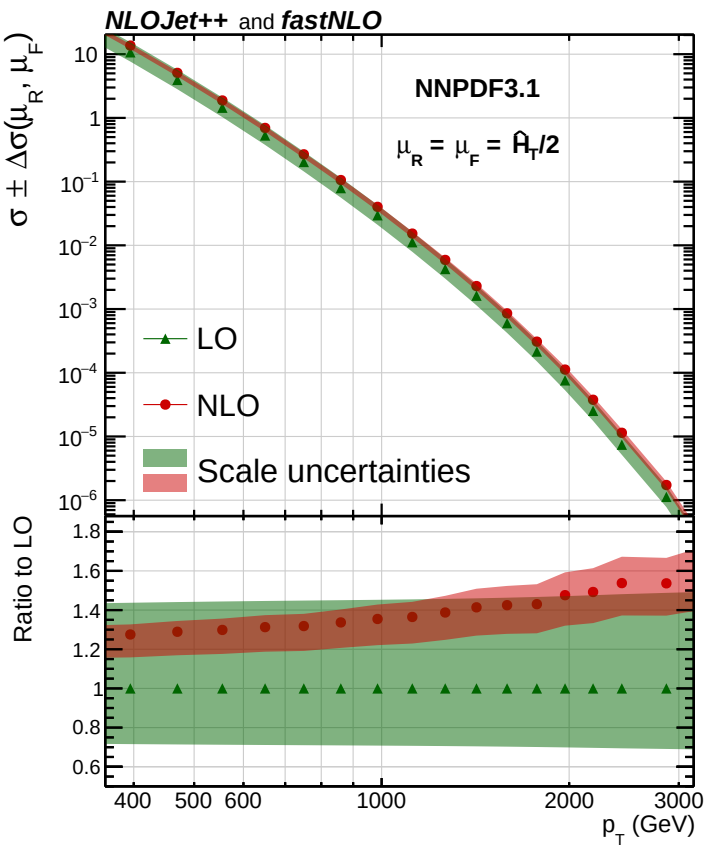

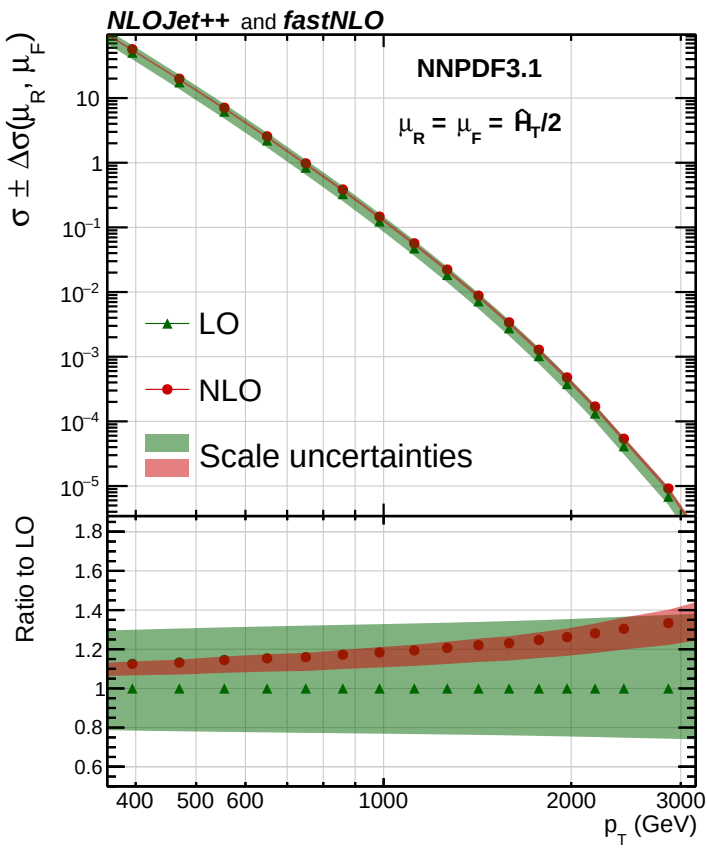

Non-Perturbative corrections

- Fixed order QCD predictions are available at parton level only: non-perturbative (NP) corrections account for multiple parton interactions (MPI) and hadronization (HAD):

Non-Perturbative corrections

- Fixed order QCD predictions are available at parton level only: non-perturbative (NP) corrections account for multiple parton interactions (MPI) and hadronization (HAD):
  - NP correction factors: $\boxed{C^{\mathrm{NP}} = \dfrac{\sigma^{\mathrm{PS+MPI+HAD}}}{\sigma^{\mathrm{PS}}}}$
  - Simple polynomial function $a + b \cdot p_T^c$ for the parametrization of C^{NP}.
  - Envelope from the predictions of the different MC event generators.

Non-Perturbative corrections

- Fixed order QCD predictions are available at parton level only: non-perturbative (NP) corrections account for multiple parton interactions (MPI) and hadronization (HAD):
  - NP correction factors: $$C^{\mathrm{NP}} = \frac{\sigma^{\mathrm{PS+MPI+HAD}}}{\sigma^{\mathrm{PS}}}$$
  - Simple polynomial function $a + b \cdot p_T^c$ for the parametrization of C^{NP}.
  - Envelope from the predictions of the different MC event generators.

C^{NP} for numerator of $R_{\Delta\phi}$

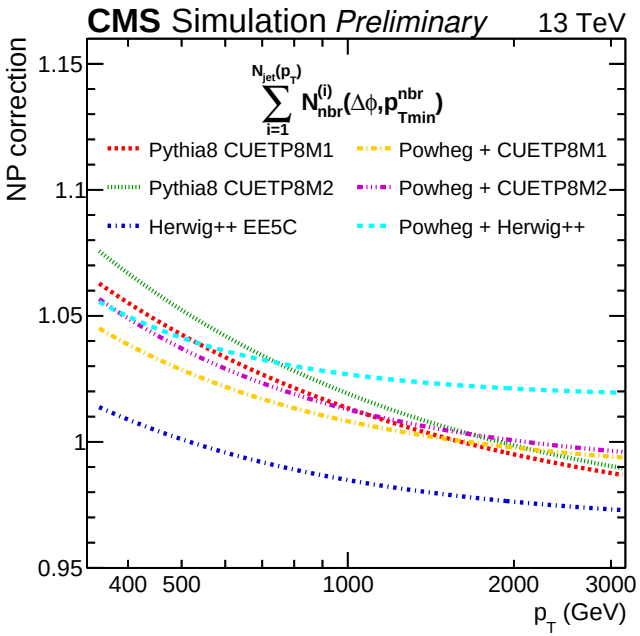

C^{NP} for denominator of $R_{\Delta\phi}$

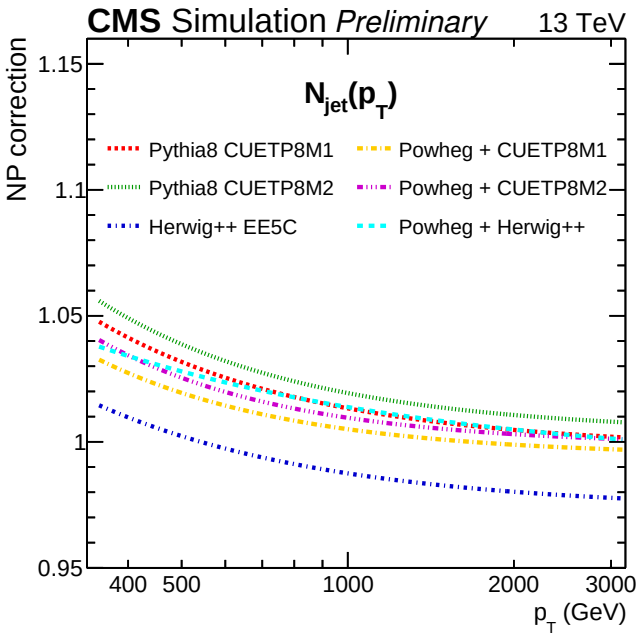

C^{NP} for $R_{\Delta\phi}$

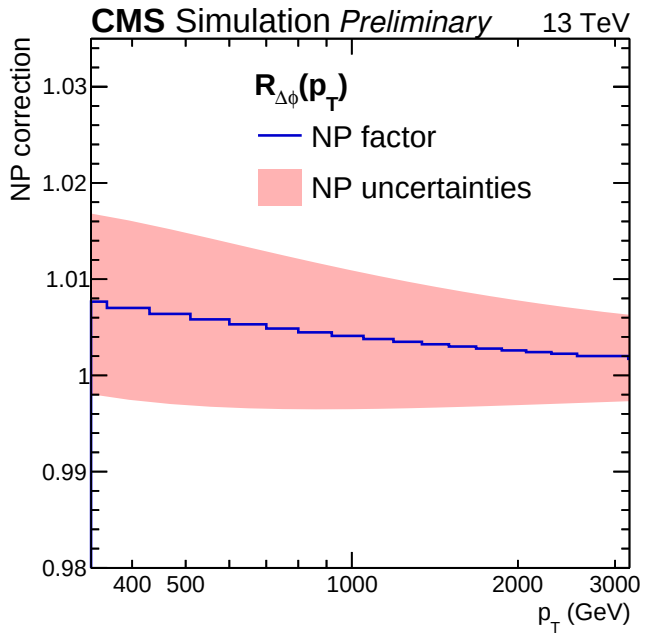

ElectroWeak corrections

- Theoretical predictions are also corrected for the **E**lectro**W**eak (EW) effects.
- Full NLO corrections to 3-jet production at the LHC ▸ arxiv:1902.01763
  $\mathcal{O}(\alpha_s^n \alpha^m)$, with $n + m = 2$ and $n + m = 4$.

ElectroWeak corrections

- Theoretical predictions are also corrected for the **E**lectro**W**eak (EW) effects.
- Full NLO corrections to 3-jet production at the LHC ▸ arxiv:1902.01763 $\mathcal{O}(\alpha_s^n \alpha^m)$, with $n+m=2$ and $n+m=4$.

Corrections formulation

Pure NLO EW corrections for n-jet:

$$\sigma_{nj}^{\text{NLO EW}} = \sigma_{nj}^{\text{LO}} + \sigma_{nj}^{\Delta\text{NLO}_1}$$

ΔNLO_1: virtual and real EW corrections.

Combination to QCD process:

1. **Additive:** $\sigma_{nj}^{\text{NLO QCD+EW}}$

$$\sigma_{nj}^{\text{LO}} + \sigma_{nj}^{\Delta\text{NLO}_0} + \sigma_{nj}^{\Delta\text{NLO}_1}$$

ΔNLO_0: virtual and real QCD corrections.

2. **Multiplicative:** $\sigma_{nj}^{\text{NLO QCD}\times\text{EW}}$

$$\sigma_{nj}^{\text{LO}} \left(1 + \frac{\sigma_{nj}^{\Delta\text{NLO}_0}}{\sigma_{nj}^{\text{LO}}}\right) \left(1 + \frac{\sigma_{nj}^{\Delta\text{NLO}_1}}{\sigma_{nj}^{\text{LO}}}\right)$$

ElectroWeak corrections

- Theoretical predictions are also corrected for the **E**lectro**W**eak (EW) effects.
- Full NLO corrections to 3-jet production at the LHC ▸ arxiv:1902.01763
  $\mathcal{O}(\alpha_s^n \alpha^m)$, with $n+m=2$ and $n+m=4$.

Corrections formulation

Pure NLO EW corrections for n-jet:

$$\sigma_{nj}^{\text{NLO EW}} = \sigma_{nj}^{\text{LO}} + \sigma_{nj}^{\Delta\text{NLO}_1}$$

ΔNLO_1: virtual and real EW corrections.

Combination to QCD process:

1. **Additive:** $\sigma_{nj}^{\text{NLO QCD+EW}}$

$$\sigma_{nj}^{\text{LO}} + \sigma_{nj}^{\Delta\text{NLO}_0} + \sigma_{nj}^{\Delta\text{NLO}_1}$$

ΔNLO_0: virtual and real QCD corrections.

2. **Multiplicative:** $\sigma_{nj}^{\text{NLO QCD}\times\text{EW}}$

$$\sigma_{nj}^{\text{LO}} \left(1 + \frac{\sigma_{nj}^{\Delta\text{NLO}_0}}{\sigma_{nj}^{\text{LO}}}\right)\left(1 + \frac{\sigma_{nj}^{\Delta\text{NLO}_1}}{\sigma_{nj}^{\text{LO}}}\right)$$

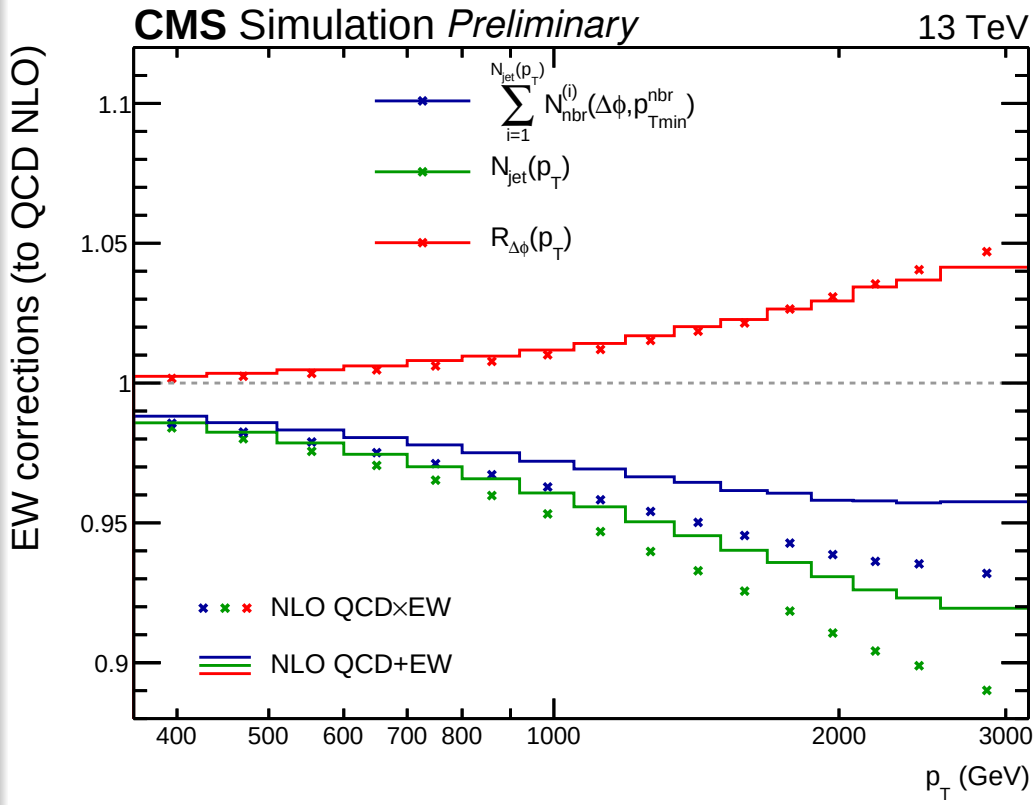

EW corrections for $R_{\Delta\phi} < 5\%$.
EW correction uncertainties $< 0.6\%$.

Determination of $\alpha_S(M_Z)$

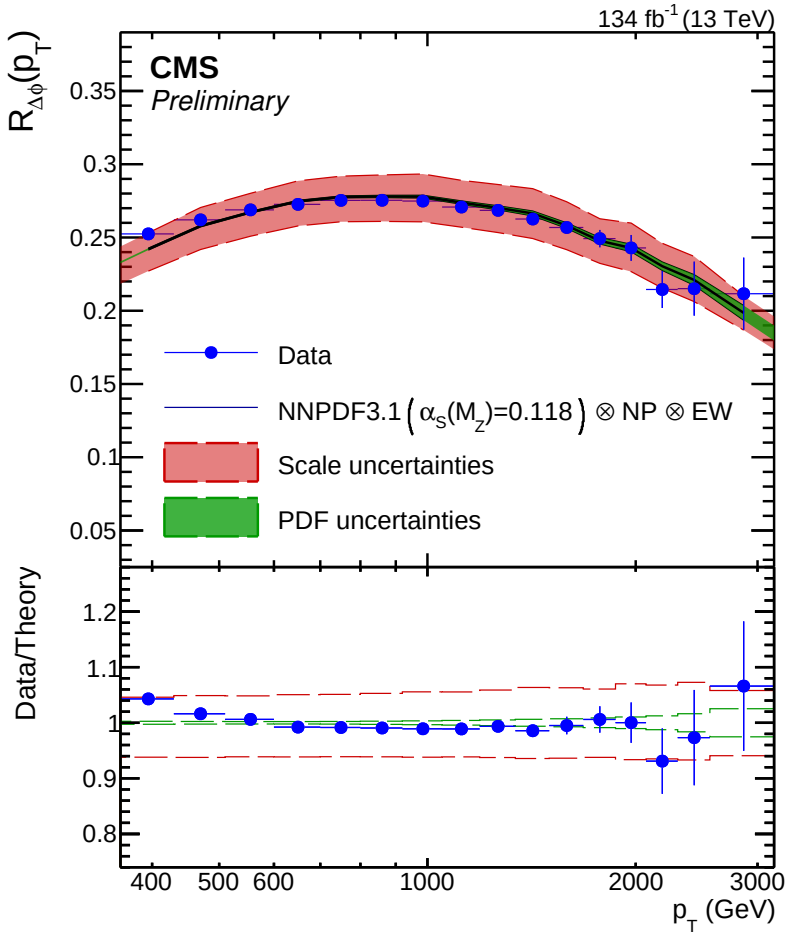

- Data-theory agreement (within the uncertainties) for all the PDF sets.
- PDF uncertainties: 1-2%.
- Scale uncertainties: 2-8%.

Determination of $\alpha_S(M_Z)$

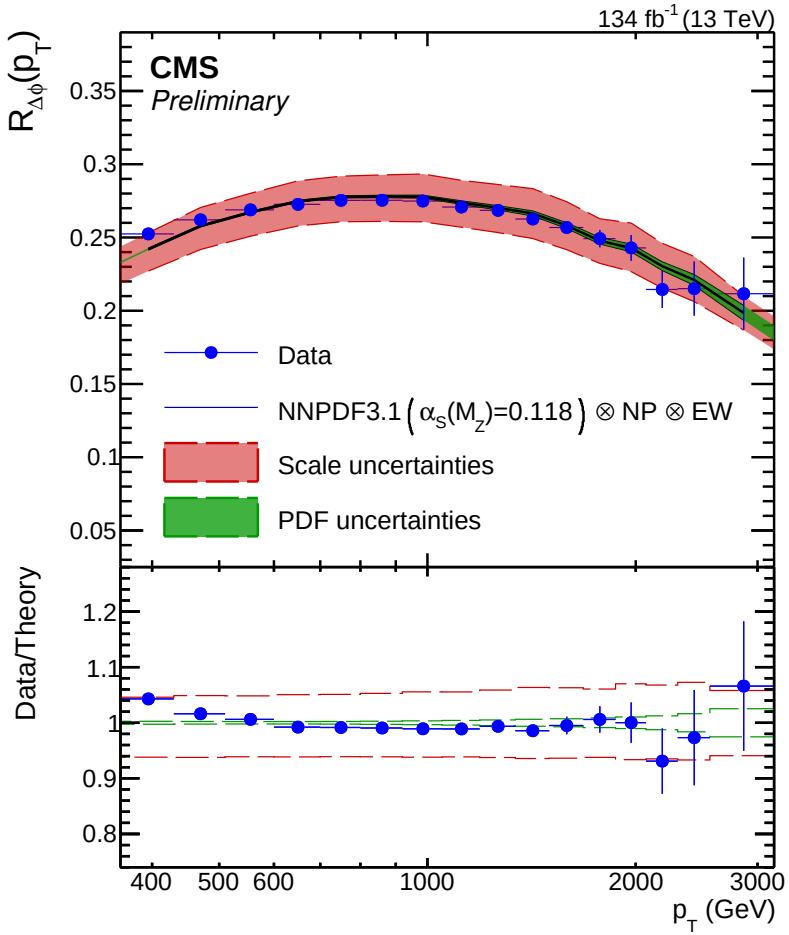

- Data-theory agreement (within the uncertainties) for all the PDF sets.
- PDF uncertainties: 1-2%.
- Scale uncertainties: 2-8%.

Determination of $\alpha_S(M_Z)$

- **Minimization of:**

$$\chi^2 = \sum_{ij}^{N} (D_i - T_i) C_{ij}^{-1} (D_j - T_j)$$

N: number of measurements
D_i: experimental data
T_i: theoretical predictions
C_{ij}: covariance matrix

- **Covariance matrix composition:**

$$C_{ij} = C_{uncor} + C_{exp} + C_{theo}$$

C_{uncor}: numerical precision of FO predictions
C_{exp}: all the experimental uncertainties
C_{theo}: all the theoretical uncertainties

Determination of $\alpha_S(M_Z)$

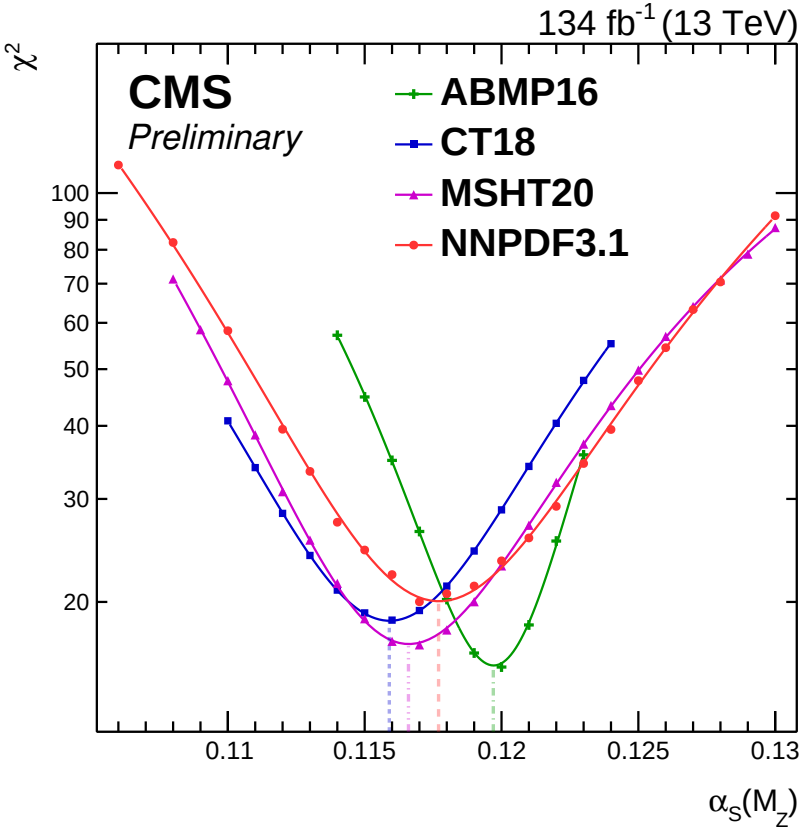

PDF set	$\alpha_S(M_Z)$	Exp	NP	PDF	EW	Scale	Total	χ^2/n_{dof}
ABMP16	0.1197	0.0008	0.0007	0.0007	0.0002	$^{+0.0043}_{-0.0042}$	$^{+0.0045}_{-0.0044}$	16/16
CT18	0.1159	0.0013	0.0009	0.0014	0.0002	$^{+0.0099}_{-0.0067}$	$^{+0.0101}_{-0.0070}$	19/16
MSHT20	0.1166	0.0013	0.0008	0.0010	0.0003	$^{+0.0112}_{-0.0063}$	$^{+0.0114}_{-0.0066}$	17/16
NNPDF3.1	0.1177	0.0013	0.0011	0.0010	0.0003	$^{+0.0114}_{-0.0068}$	$^{+0.0116}_{-0.0071}$	20/16

Determination of $\alpha_S(M_Z)$

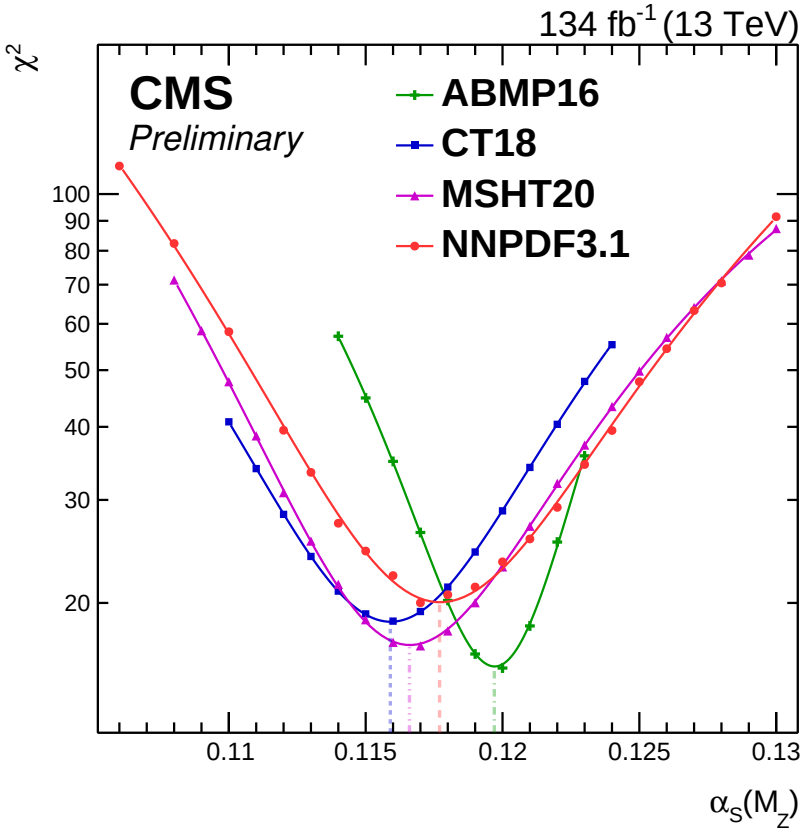

PDF set	$\alpha_S(M_Z)$	Exp	NP	PDF	EW	Scale	Total	χ^2/n_{dof}
ABMP16	0.1197	0.0008	0.0007	0.0007	0.0002	$^{+0.0043}_{-0.0042}$	$^{+0.0045}_{-0.0044}$	16/16
CT18	0.1159	0.0013	0.0009	0.0014	0.0002	$^{+0.0099}_{-0.0067}$	$^{+0.0101}_{-0.0070}$	19/16
MSHT20	0.1166	0.0013	0.0008	0.0010	0.0003	$^{+0.0112}_{-0.0063}$	$^{+0.0114}_{-0.0066}$	17/16
NNPDF3.1	0.1177	0.0013	0.0011	0.0010	0.0003	$^{+0.0114}_{-0.0068}$	$^{+0.0116}_{-0.0071}$	20/16

- Scale uncertainties by far the dominant: 4-10%.
- All the $\alpha_s(M_Z)$ are compatible among each other.

Determination of $\alpha_S(M_Z)$

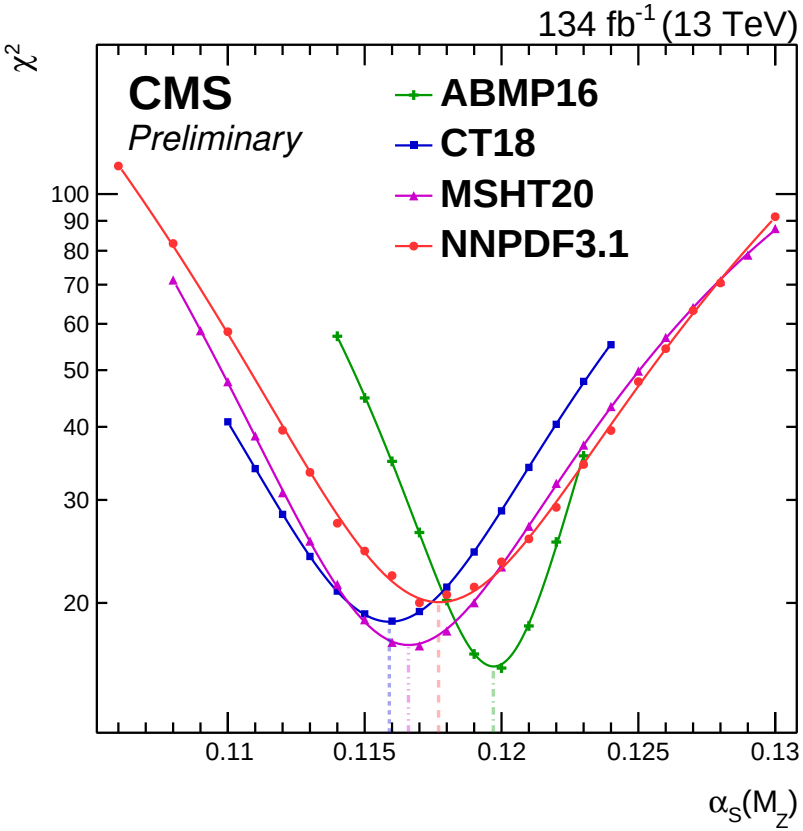

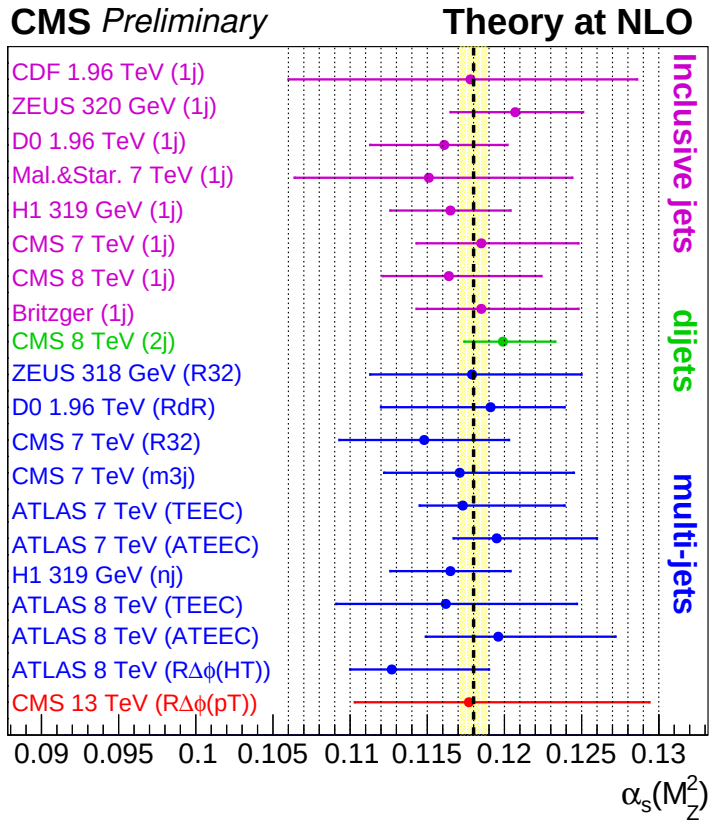

PDF set	$\alpha_S(M_Z)$	Exp	NP	PDF	EW	Scale	Total	χ^2/n_{dof}
ABMP16	0.1197	0.0008	0.0007	0.0007	0.0002	$^{+0.0043}_{-0.0042}$	$^{+0.0045}_{-0.0044}$	16/16
CT18	0.1159	0.0013	0.0009	0.0014	0.0002	$^{+0.0099}_{-0.0067}$	$^{+0.0101}_{-0.0070}$	19/16
MSHT20	0.1166	0.0013	0.0008	0.0010	0.0003	$^{+0.0112}_{-0.0063}$	$^{+0.0114}_{-0.0066}$	17/16
NNPDF3.1	0.1177	0.0013	0.0011	0.0010	0.0003	$^{+0.0114}_{-0.0068}$	$^{+0.0116}_{-0.0071}$	20/16

- Results also compatible with the world average: $\alpha_s(M_Z) = 0.1180 \pm 0.0009$.

$\alpha_S(Q)$ evolution

1. Split the p_T range into 4 sub-regions.

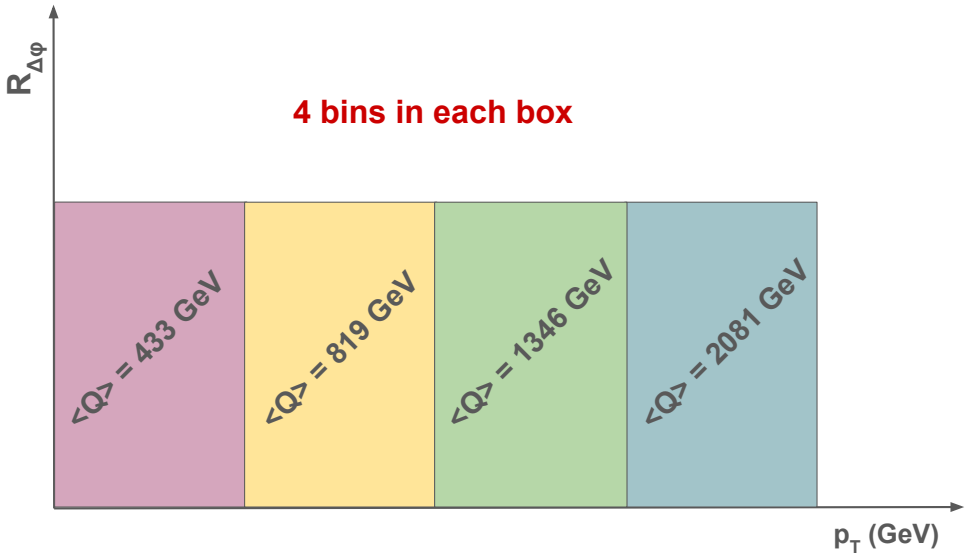

$\alpha_S(Q)$ evolution

1. Split the p_T range into 4 sub-regions.
2. Determination of the $\alpha_s(M_Z)$ in each sub-region independently.

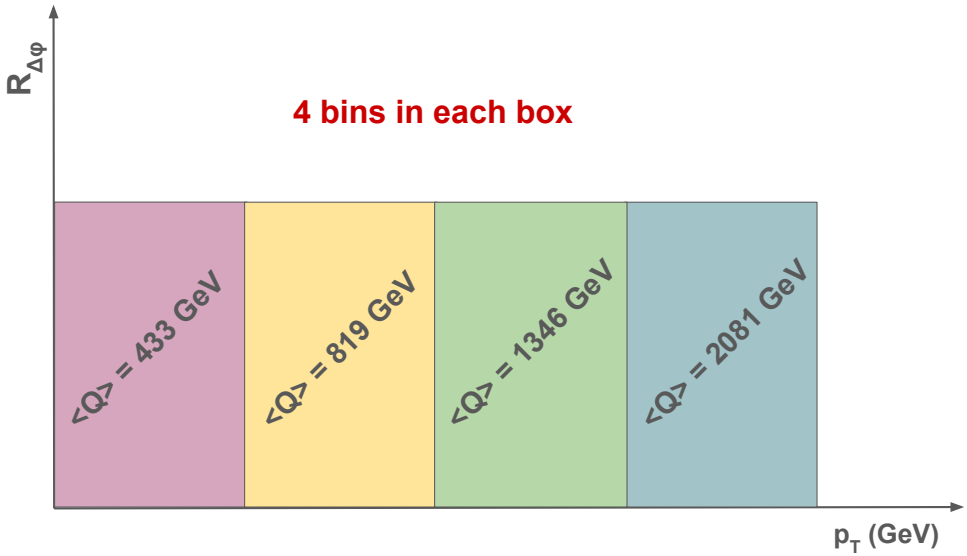

$\alpha_S(Q)$ evolution

1. Split the p_T range into 4 sub-regions.
2. Determination of the $\alpha_s(M_Z)$ in each sub-region independently.
3. Calculation of the cross-section-weighted average $\langle Q \rangle$ for each sub-region.
4. The $\alpha_s(M_Z)$ values are evolved to $\alpha_s(Q)$, using the RGE.

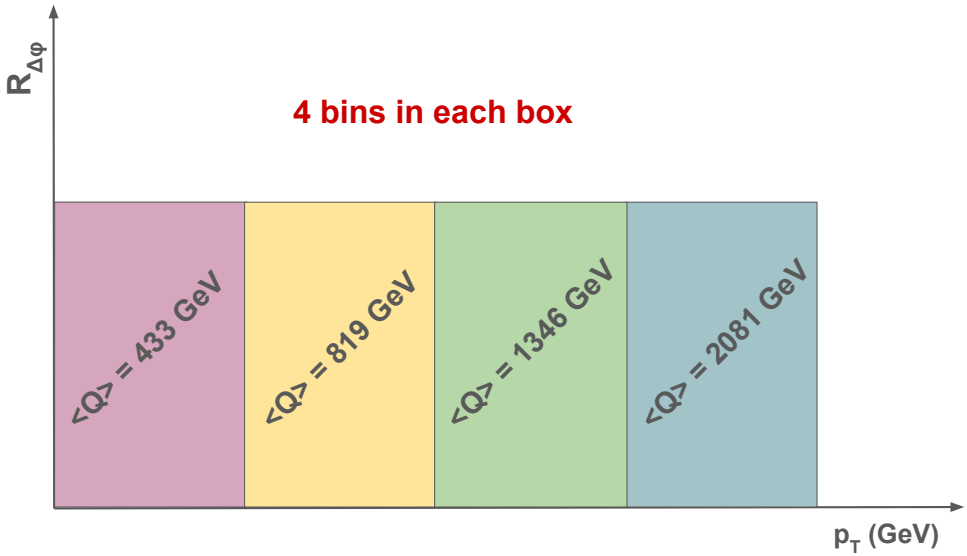

p_T range (GeV)	$\alpha_S(M_Z)$	$\langle Q \rangle$ (GeV)	$\alpha_S(Q)$
$360 - 700$	$0.1177^{+0.0104}_{-0.0067}$	433.0	$0.0967^{+0.0066}_{-0.0044}$
$700 - 1190$	$0.1162^{+0.0108}_{-0.0073}$	819.0	$0.0878^{+0.0060}_{-0.0042}$
$1190 - 1870$	$0.1159^{+0.0112}_{-0.0077}$	1346.0	$0.0830^{+0.0055}_{-0.0040}$
$1870 - 3170$	$0.1118^{+0.0110}_{-0.0070}$	2081.0	$0.0775^{+0.0051}_{-0.0034}$

$\alpha_S(Q)$ evolution

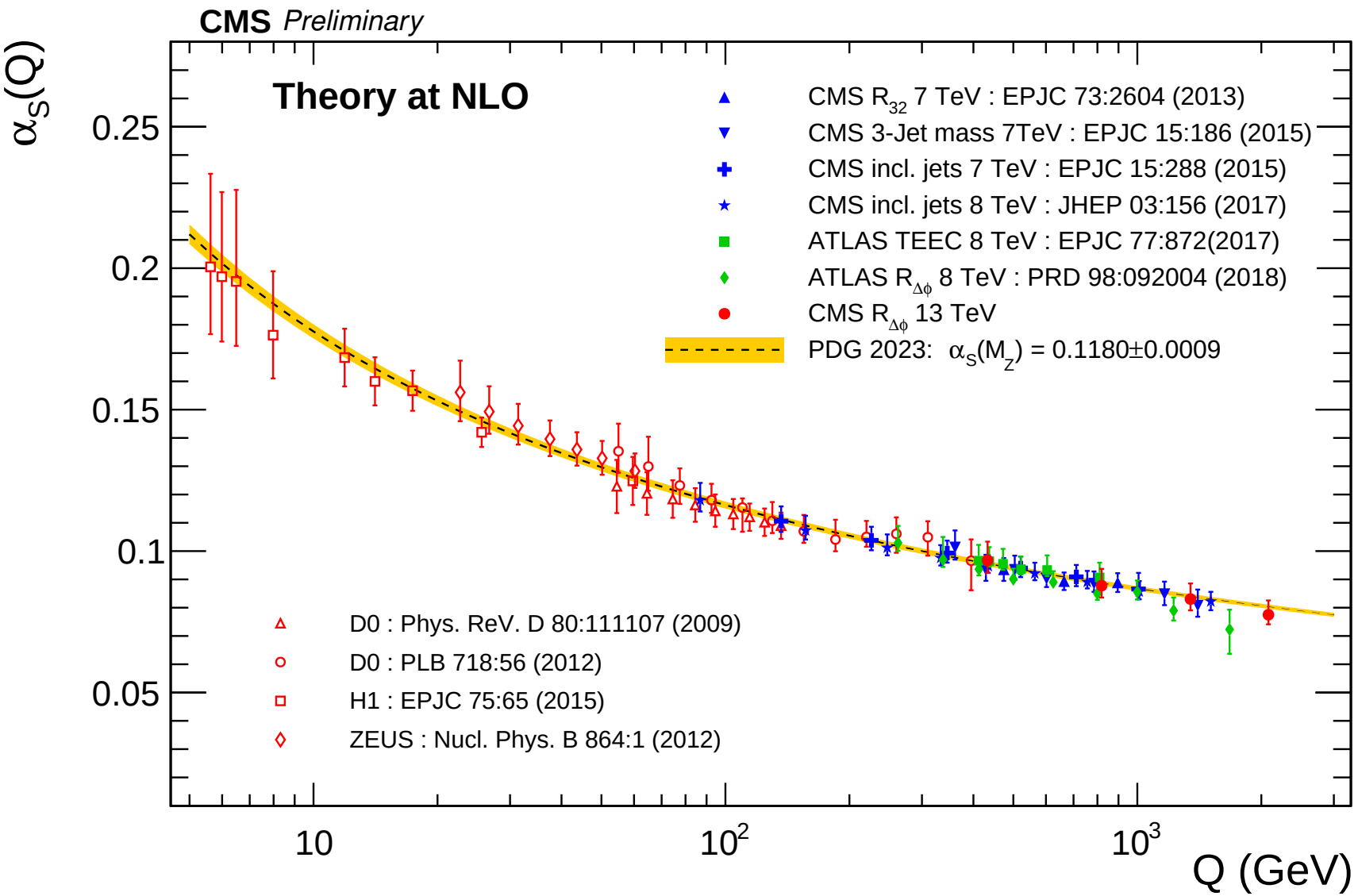

All the analysis results are consistent with the energy dependence predicted by the RGE and no deviation is observed up to $\sim$ 2 TeV.

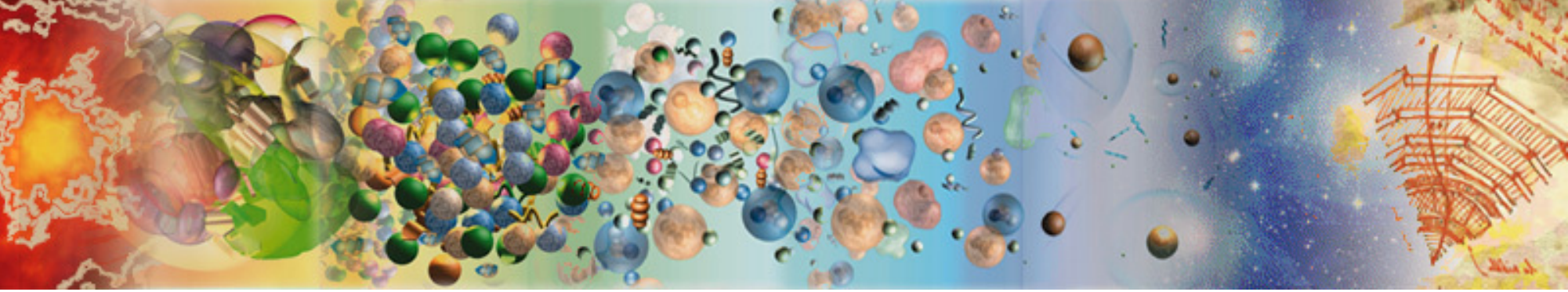

THANK YOU FOR YOUR ATTENTION